



Article citation information:

Margielewicz, J., Gąska, D., Wojnar, G. Numerical modelling of toothed gear dynamics. *Scientific Journal of Silesian University of Technology. Series Transport*. 2017, **97**, 105-115. ISSN: 0209-3324. DOI: <https://doi.org/10.20858/sjsutst.2017.97.10>.

Jerzy MARGIELEWICZ¹, Damian GAŚKA², Grzegorz WOJNAR³

NUMERICAL MODELLING OF TOOTHED GEAR DYNAMICS

Summary. This paper presents the results of computer simulations of a gear model, where the variable stiffness of the meshing and backlash are considered. The outcome of such assumptions is a non-linear mathematical model in which chaotic phenomena can occur. During model studies, attention was paid to the identification of areas limited by the physical parameters, for which the analysed system behaved chaotically. To determine the ranges of irregular gear behaviour, numerical procedures were used to plot the bifurcation diagram, the Lyapunov exponent, the amplitude-frequency distribution and the Poincaré cross section.

Keywords: dynamics; non-linear vibrations; chaos; toothed gear

1. INTRODUCTION

Heavy-duty machines, in particular cranes, perform complex tasks with the result that heavy loads are transported at close range. When transporting a load, it often happens that the operator is forced to manoeuvre it to avoid collisions with surrounding obstacles. Making safe manoeuvres is not possible without properly functioning enforcement mechanisms. In every mechanism, there are toothed gears whose primary purpose is to transform mechanical energy

¹ Faculty of Transport, Silesian University of Technology, Krasińskiego 8 Street, 40-019 Katowice, Poland.
E-mail: jerzy.margielewicz@polsl.pl.

² Faculty of Transport, Silesian University of Technology, Krasińskiego 8 Street, 40-019 Katowice, Poland.
E-mail: damian.gaska@polsl.pl.

³ Faculty of Transport, Silesian University of Technology, Krasińskiego 8 Street, 40-019 Katowice, Poland.
E-mail: grzegorz.wojnar@polsl.pl.

by reducing or multiplying angular speed. Reducers used in crane hoisting mechanisms, whose ratios are in the range of $32 \div 100$, are usually performed in three stages. However, in the range of ratios from $112 \div 450$, they are performed in four stages. Depending on the manufacturer, two-speed gearboxes with gear ratios of $7 \div 50$ are also used in the mechanisms. Such large gears allow for lifting loads up to $500 t$. The typical range of crane-hoisting capacity ranges from $5 \div 50 t$. The nominal torque at the gearbox output with gear ratios from $7 \div 450$ is in the range of $12 \div 660 kNm$. Single-stage gear units can also be used in low-level hoisting mechanisms.

The free meshing of the wheels is ensured by the backlash and bottom clearance [17]. Their presence is one of the main sources behind non-linearities appearing. Since the mid-20th century there has been a growing interest among researchers in the dynamics of non-linear systems [3,8,9]. Non-linearities cause irregular intermittent forces in the gearboxes. It is believed that a given phenomenon is chaotic if it is characterized by high irregularities. Chaotic dynamics are evident when, in a two-run system, trajectories initially located nearby expire exponentially over time [3]. Most commonly used in computer simulations, gear models are based on non-linear differential equations with variable coefficients. In gearing, the variation of coefficients is mainly due to the stiffness of the meshing, which depends on the number of pairs of teeth in the tooth contact. It is worth mentioning that the ratio of stiffness of two-way and one-way meshing is usually in the range of 1.7 to 2 [16]. Its value depends, inter alia, on the transmission ratio and the values of the shift coefficients [11,18,23]. The source of the excited vibrations of the cooperating pair of gear wheels is also a deviation in the design and the position. Mostly, they are caused by radial run-out and deviation in the tooth profile from the ideal position [15]. They are also often mapped via a function that is a superposition of several harmonic components [7,22]. Mathematical models of toothed gears, in addition to stiffness of the gearing, also take into account the susceptibility to roller bearings on which the gears are mounted [25].

Studies of non-linear gear models also deal with issues related to chaos. These analyses, inter alia, concern the influence of individual parameters on the dynamics of the transmission [1,10,14,21]. In performed numerical experiments, the qualitative influence of the parameters of the mathematical model characterizing single-stage gear on its dynamics was investigated. To identify areas where chaos may have occurred, bifurcation diagrams and charts of the maximum Lyapunov exponent were created. It is believed that Lyapunov's maximum exponent is one of the more reliable indicators for evaluating the chaotic system, as its positive values indicate the irregular behaviour of the system under study [2]. From a theoretical point of view, Lyapunov exponents measure the sensitivity of the studied system towards initial conditions and are interpreted as the average rate of dissipation along the trajectory in the phase plane [4]. The bifurcation diagrams provide quantitative and qualitative information on the doubling of the period, while the qualitative properties are most conveniently investigated by fractal geometry [19]. In this sense, it is worth mentioning that the term 'bifurcation', within chaos theory, is understood as the division of the path of solutions [13].

2. FORMULATION OF THE MATHEMATICAL MODEL OF SINGLE-STAGE GEARING

Gears with straight teeth were modelled as a mechanical vibration system with two degrees of freedom. The formulated model consists of two non-deformable discs with radii R_1 and R_2 ,

whose inertial properties are mass moments of inertia J_1 and J_2 . The discs rotate relative to the rigidly supported axis of rotation O_1 and O_2 . The forces generated in the engagement of the mating wheels are mapped in parallel onto the joint of the spring c_z element and dispersing element b_z . In addition, backlash $2L_z$ and the static error of the gearwheel cooperation $e(t)$ have been considered. In model studies, the gear wheel cooperation error is treated as a kinematic effect on the cooperating teeth. The transmission is induced by the external torque M_1 , while the resistance torque also affects the M_2 gear. During the formulation of the phenomenological model, the influence of errors caused by the positioning and the execution of the gears was omitted.

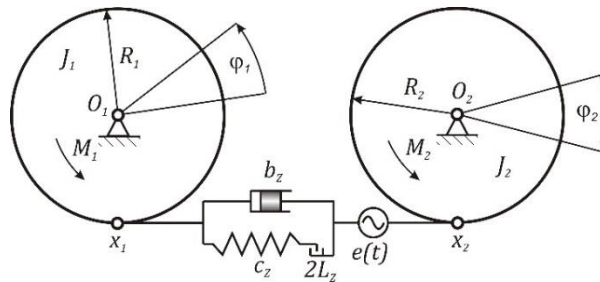


Fig. 1. Model of a toothed gear

Based on the phenomenological model, differential equations of motion have been derived, which ultimately take on the following form:

$$\begin{cases} J_1 \ddot{\varphi}_1 + b_z R_1 (R_1 \dot{\varphi}_1 - R_2 \dot{\varphi}_2 - \dot{e}(t)) + c_z R_1 (R_1 \varphi_1 - R_2 \varphi_2 - e(t)) f(q) = M_1, \\ J_2 \ddot{\varphi}_2 - b_z R_2 (R_1 \dot{\varphi}_1 - R_2 \dot{\varphi}_2 - \dot{e}(t)) - c_z R_2 (R_1 \varphi_1 - R_2 \varphi_2 - e(t)) f(q) = -M_2. \end{cases} \quad (1)$$

It is more convenient to evaluate the nature of the forces generated in meshing by using a reduced model with one degree of freedom:

$$m_{red} \ddot{q} + b_z \dot{q} + c_z(t) f(q, L_z) = F_{sr} + F_s, \quad (2)$$

where:

$$q = R_1 \varphi_1 - R_2 \varphi_2, \quad c_z q = c_z(t) f(q, L_z), \quad e(t) = e_1 \cos(\omega_z t), \\ m_{red} = \frac{J_1 J_2}{J_2 R_1^2 + J_1 R_2^2}, \quad F_{sr} = \frac{J_1 J_2}{J_2 R_1^2 + J_1 R_2^2} \left(\frac{R_1 M_1}{J_1} + \frac{R_2 M_2}{J_2} \right), \quad F_s = \frac{J_1 J_2 \ddot{e}(t)}{J_2 R_1^2 + J_1 R_2^2},$$

$\omega_z = z_1 \cdot \omega_s$ - frequency of meshing, ω_s - angular velocity of the motor, and z_1 - number of pinion teeth.

The variable stiffness of meshing plays a significant influence on the value of the forces acting on the gear teeth, but is not a source of non-linearity. The main cause of non-linearity, which occurs in numerical gear models, is the backlash $2L_z$. Its presence ensures that the meshing wheels are free to mesh and demesh. Most often, it is modelled using non-linear functions with a so-called dead zone [12,24]:

$$f(q, L_z) = \begin{cases} q + L_z, & q < -L_z, \\ 0, & -L_z \leq q \leq L_z, \\ q - L_z, & q > L_z. \end{cases} \quad (3)$$

The simplest and least laborious way to identify stiffness in a tooth is to treat it as a fixed beam. This approach provides imprecise results, but can be used to perform initial computer simulations. This approach calculates the angular displacement of the gear wheel caused by the force acting on the gear tooth [20]. With this information, it is still possible to estimate the average rigidity of one- and two-way meshes by the following relationships:

$$c_{Z1} = \frac{M_N}{R_1^2 \Delta\varphi_I'}, \quad c_{Z2} = \frac{M_N}{R_2^2 \Delta\varphi_{II}'} \quad (4)$$

where:

$\Delta\varphi_I'$ - angular displacement of the wheel at one-way mesh, and $\Delta\varphi_{II}'$ - angular displacement of the wheel at two-way mesh.

Based on the above, and using the Cai formula [5,6], the variable stiffness of time function is obtained. Modelling dynamic systems, whose properties are described by discontinuous functions, is cumbersome. Considering the improvement in numerical calculations, variable meshing stiffness is reproduced through the harmonic function:

$$c_z(t) = c_0 + c_1 \cos(\omega_z t), \quad (5)$$

where:

c_0 - medium meshing stiffness, and c_1 - amplitude of the dynamic component.

To more accurately reproduce variable meshing stiffness in the computer simulation, the discontinuous functions shown in Fig. 2 can be expanded into a Fourier series. In view of the efficient and effective conduct of numerical experiments, the mathematical model in (2) was written in dimensionless form:

$$\ddot{u} + 2h\dot{u} + [1 + \alpha \cos(\omega\tau)]f(u) = f_{\dot{s}r} + f_s \omega^2 \cos(\omega\tau), \quad (6)$$

where:

$$\omega_0 = \sqrt{\frac{c_0}{m_{red}}}, \quad h = \frac{b_z}{2\sqrt{m_{red}c_0}}, \quad \alpha = \frac{c_1}{c_0}, \quad \omega = \frac{\omega_z}{\omega_0}, \quad f_{\dot{s}r} = \frac{F_{\dot{s}r}}{L_z c_0}, \quad f_s = \frac{F_s}{L_z}, \quad u = \frac{q}{L_z}.$$

The consequence of dimensionless writing and the introduction of a new coordinate represents the change in the dead zone range, which is currently in the range of $-l$ to l . Transforming the mathematical model of a toothed gear in (2) to form (6) significantly accelerates numerical calculations. This formulated mathematical model is the formal basis for quantitative and qualitative computer simulations.

3. MODEL TESTS OF A TOOTHED GEAR

Sample model tests were carried out, based on numerical data specifying a single-stage gear (Table 1). Model studies were conducted using the computer program Mathematica (version 11).

Tab. 1

Parameters characterizing the analysed system

Name	Symbol	Value
Module	\hat{m}	5 [mm]
Number of wheels (1 tooth)	z_1	14
Number of wheels (2 teeth)	z_2	85
Rotor mass moment of inertia	J_S	2.7 [kg m ²]
Drum mass moment of inertia	J_B	5.3 [kg m ²]
Wheel 1: mass moment of inertia	J_1	0.0011 [kg m ²]
Wheel 2: mass moment of inertia	J_2	1.12 [kg m ²]
Medium meshing stiffness	c_0	$5.03 \cdot 10^8$ [Nm ⁻¹]
Amplitude of the dynamic component	c_1	$3.27 \cdot 10^7$ [Nm ⁻¹]
Error of the gearwheel cooperation	e_1	0.01 [mm]
Rated power of the drive motor	P	12 [kW]
Nominal speed of the drive motor	n_s	1,450 [obr/min]

When performing computer simulations in the formulated phenomenological model (Fig. 1), the inertia of the electric motor rotor J_S and the rope winch drum J_B were considered. The obtained results of numerical calculations illustrating the influence of particular parameters of the mathematical model on the dynamics of gears are presented in the form of bifurcation diagrams, as well as the maximal Lyapunov exponent, the time waveform of generalized coordinates, the amplitude-frequency spectra and the Poincaré cross sections.

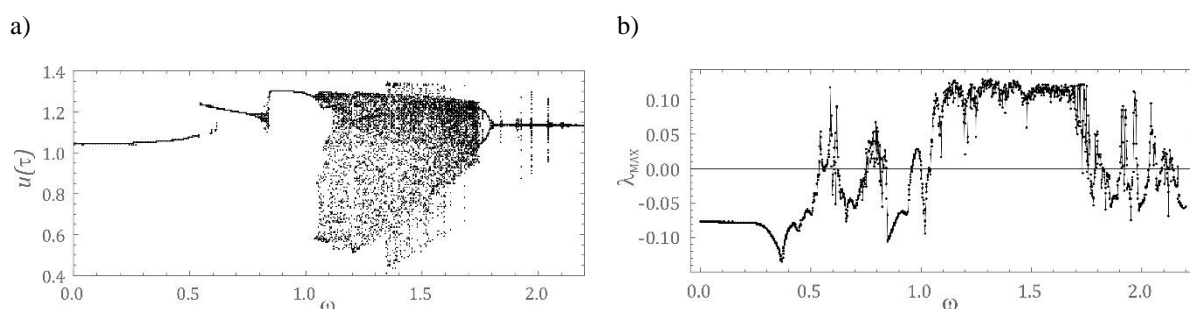


Fig. 2. Results of calculations showing the influence of frequency on system dynamics obtained on the assumption of the following parameters: $h=0.06$, $\alpha=0.065$, $f_{sr}=0.044$, $f_e=0,1$ - a) bifurcation diagram, b) maximal Lyapunov exponent

The time waveforms, amplitude-frequency spectra and Poincaré cross sections are further illustrated. However, it is limited to the illustration of strange attractors arising on the phase plane, when the value of the corresponding frequency of meshing is changed in the cooperating gear wheels.

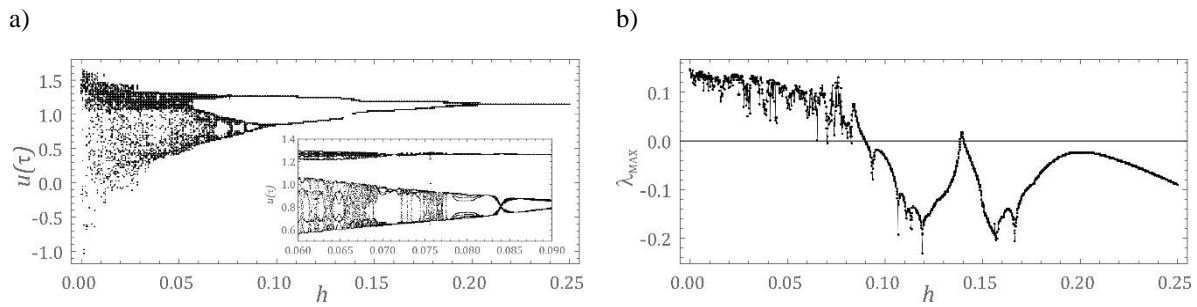


Fig. 3. Results of calculations showing the influence of frequency on system dynamics obtained on the assumption of the following parameters: $\omega \approx 1.092$, $\alpha = 0.065$, $f_{sr} = 0.044$, $f_e = 0.1$ - a) bifurcation diagram, b) maximal Lyapunov exponent

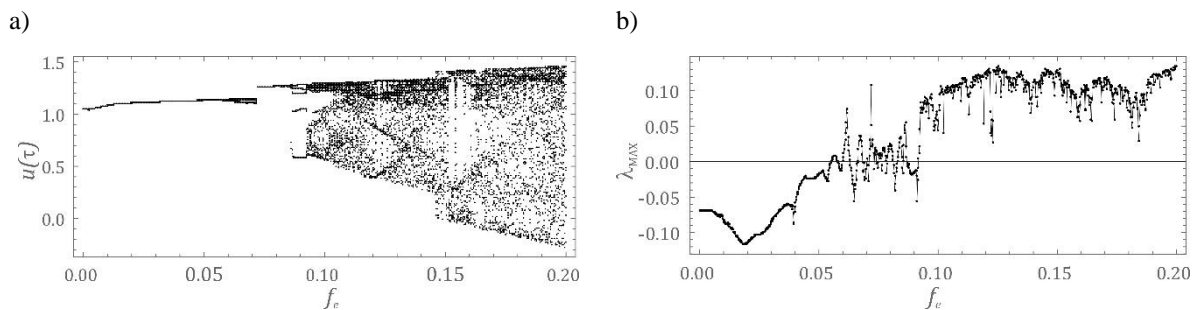


Fig. 4. Results of calculations showing the influence of frequency on system dynamics obtained on the assumption of the following parameters: $\omega \approx 1.092$, $h = 0.06$, $\alpha = 0.065$, $f_{sr} = 0.044$ - a) bifurcation diagram, b) maximal Lyapunov exponent

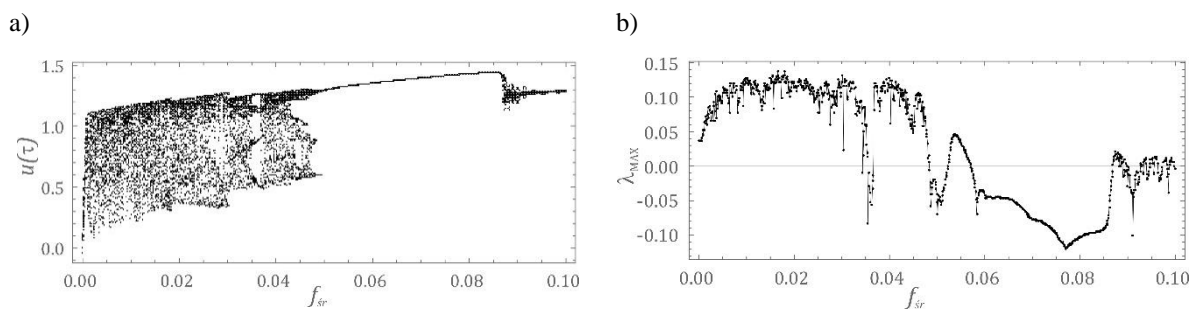


Fig. 5. Results of calculations showing the influence of frequency on system dynamics obtained on the assumption of the following parameters: $\omega \approx 1.092$, $h = 0.06$, $\alpha = 0.065$, $f_e = 0.1$ - a) bifurcation diagram, b) maximal Lyapunov exponent

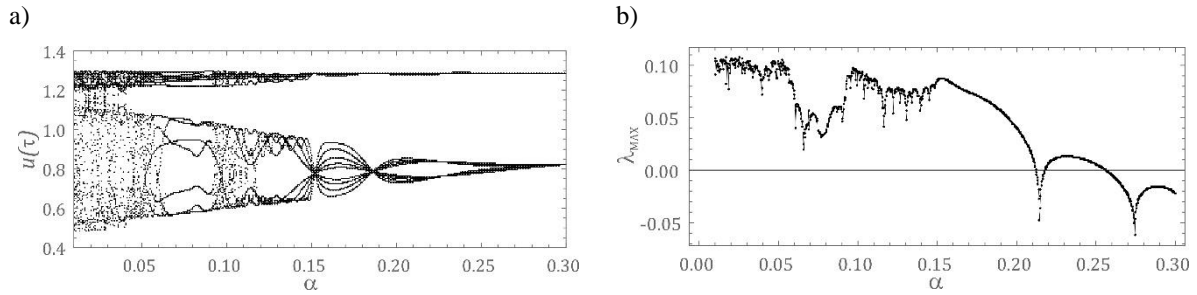


Fig. 6. Results of calculations showing the influence of frequency on system dynamics obtained on the assumption of the following parameters: $\omega \approx 1.092$, $h=0.06$, $f_{sr}=0.044$, $f_e=0.1$ - a) bifurcation diagram, b) maximal Lyapunov exponent

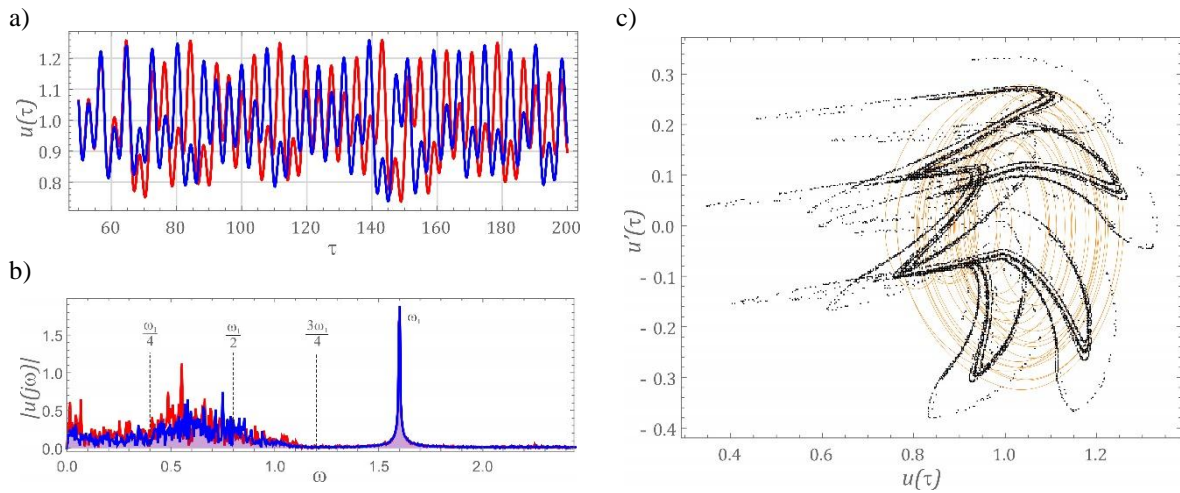


Fig. 7. Calculation results assuming the following parameters: $\omega=1.6$, $h=0.06$, $k_l=0.065$, $f_{sr}=0.044$, $f_e=0.1$ - a) the time waveform, b) amplitude-frequency spectra, c) Poincaré cross section

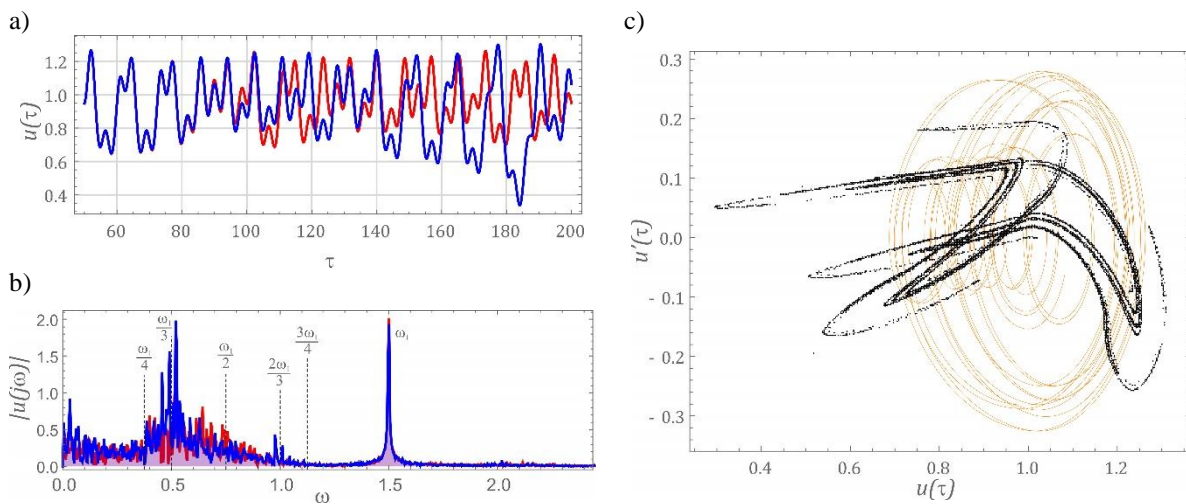


Fig. 8. Calculation results assuming the following parameters: $\omega=1.5$, $h=0.06$, $k_l=0.065$, $f_{sr}=0.044$, $f_e=0.1$ - a) the time waveform, b) amplitude-frequency spectra, c) Poincaré cross section

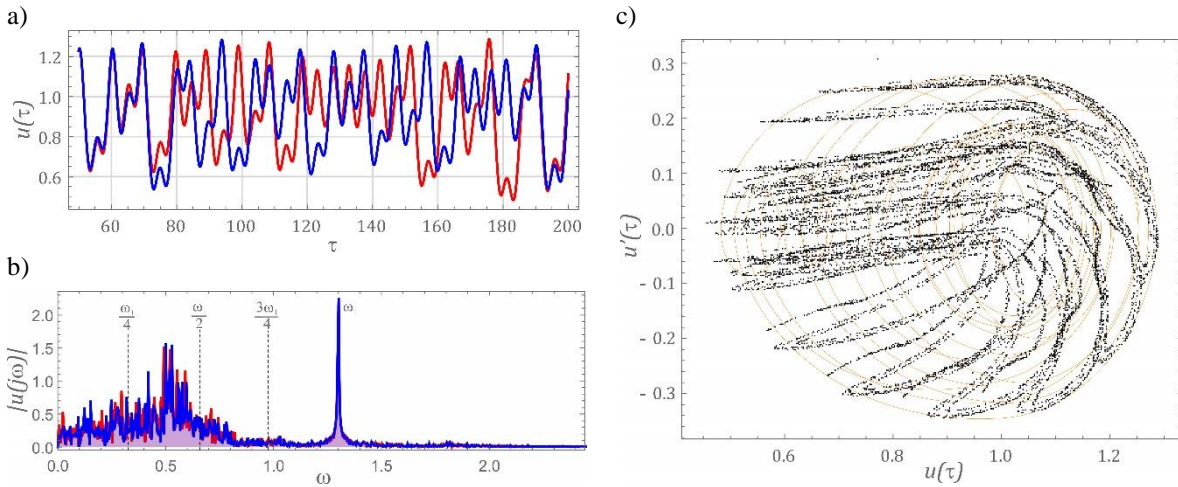


Fig. 9. Calculation results assuming the following parameters: $\omega=1.3$, $h=0.06$, $k_l=0.065$, $f_{sr}=0.044$, $f_e=0.1$ - a) the time waveform, b) amplitude-frequency spectra, c) Poincaré cross section

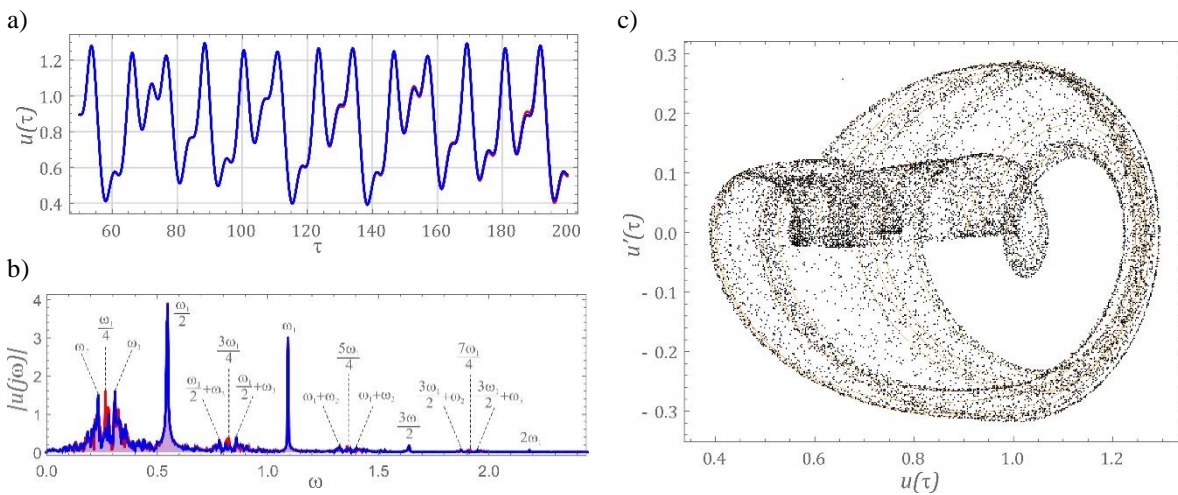


Fig. 10. Calculation results assuming the following parameters: $\omega=1.09246$, $h=0.06$, $k_l=0.065$, $f_{sr}=0.044$, $f_e=0$. 1 - a) the time waveform, b) amplitude-frequency spectra, c) Poincaré cross section

Graphs showing time waveforms and amplitude-frequency spectra also show the sensitivity of the system to the initial conditions. They were prepared with the assumption that the difference of initial displacements equalled $\varepsilon=0.0001$. To identify strange attractors, the Poincaré cross section was plotted against the background of the phase portraits.

4. ANALYSIS OF RESULTS AND CONCLUSIONS

Based on the results obtained, it was found that, when increasing the parameter f_e , representing the cooperation of the gears error, the maximum Lyapunov exponent was positive (Fig. 4). Increasing stiffness α and damping h in the meshing reduces the phenomenon of chaos (Fig. 3 and Fig. 6). A similar effect on gear dynamics involved

a parameter that characterized the external forces acting on the gear units (Fig. 5). Nevertheless, with their high values, chaotic phenomena can occur in the transmission. In the case of the frequency parameter, the chaos dominates when the meshing frequency is greater than the resonant frequency of the gear (Fig. 2). In the considered dynamic gear model, the ratio of the meshing frequency to the resonant frequency was about 1.092. This value of parameter ω did not show any noticeable sensitivity to the initial conditions (Fig. 10a). On the other hand, in the amplitude-frequency spectrum, harmonic components, which are a combination of ω_1 and ω_2 , dominate (Fig. 10b). On the basis of computer simulations, it can be stated that strange attractors appear when there are components in the amplitude-frequency spectrum corresponding to the frequency of induction $\omega = \omega_1$. In addition, the entire sequence of components up to $\frac{3}{4}\omega_1$ is excited. The shape of the strange attractor is dependent on the dominance of harmonics located in the range from $\frac{1}{4}\omega_1$ to $\frac{1}{2}\omega_1$ (Figs. 7-9). The obtained results from the model tests indicate that, when designing working machinery mechanisms, particular attention should be paid to the proper selection of the drive motor. From an operational point of view, the meshing frequency is one of the most important parameters characterizing the dynamic properties of the drive system. Its value significantly depends on the angular velocity of the impeller of the drive motor and the number of teeth. Therefore, the rotational speed should be chosen in such a way that the ratio of the meshing frequency to the resonant frequency is outside the range where the behaviour of the system is chaotic.

References

1. Al-Shyyab A., A. Kahraman. 2005. "Non-linear dynamic analysis of multi-mesh gear train using multi-term harmonics balance method: sub-harmonic motion". *Journal of Sound and Vibration* 279: 417-451. ISSN 0022-460X.
2. Awrejcewicz Jan. 1995. *Matematyczne metody mechaniki*. [In Polish: *Mathematical Methods of Mechanics*.] Łódź: Wydawnictwo Politechniki Łódzkiej. ISBN 83-86453-42-7.
3. Awrejcewicz Jan. 1997. *Tajemnice nieliniowej dynamiki*. [In Polish: *Secrets of Non-linear Dynamics*.] Łódź: Wydawnictwo Politechniki Łódzkiej. ISBN 83-87198-07-2.
4. Baker Gregory, Gollub Jerry. P. 1998. *Wstęp do dynamiki układów chaotycznych*. [In Polish: *Introduction to the Dynamics of Chaotic Systems*.] Warsaw: PWN. ISBN: 8301126175
5. Cai Y. 1995. "Simulation on the rotational vibration of helical gears in consideration of the tooth separation phenomenon". *Journal of Mechanical Design* 117: 460-469. ISSN 1050-0472. DOI:10.1115/1.2826701.
6. Cai Y., T. Hayashi. 1994. "The linear approximated equation of vibration of a pair of spur gears". *Journal of Mechanical Design* 116: 558-564. ISSN 1050-0472. DOI: 10.1115/1.2919414.
7. Ghosh S., G. Chakraborty. 2016. "On optimal tooth profile modification for reduction of vibration and noise in spur gear pairs". *Mechanism and Machine Theory* 105: 145-163. ISSN 0094-114X.
8. Grega Robert, et al., 2017. "Failure analysis of driveshaft of truck body caused by vibrations". *Engineering Failure Analysis* 79: 208-215. ISSN 1350-6307.
9. Grega Robert, et al. 2017. "Optimization of noisiness of mechanical system by using a pneumatic tuner during a failure of piston machine". *Engineering Failure Analysis* 79: 845-851. ISSN 1350-6307.

10. Jingyue W., G. Lixin, W. Haotian. 2013. "Analysis of bifurcation and nonlinear control for chaos in gear transmission system". *Research Journal of Applied Sciences, Engineering and Technology* 6 (10): 1818-1824. ISSN 2040-7459.
11. Jyoti D. Darbari, Vernika Agarwal, Venkata S.S. Yadavalli, Diego Galar, Prakash C. 2017. „A multi-objective fuzzy mathematical approach for sustainable reverse supply chain configuration”. *Journal of Transport and Supply Chain Management* 11: 1-12. DOI: 10.4102/jtscm.v11i0.267.
12. Kokare D. K., S.S. Patil. 2014. "Numerical analysis of vibration in mesh stiffness for spur gear pair with method of phasing". *International Journal of Current Engineering and Technology*, Special Issue: 156-159. ISSN 2277 - 4106.
13. Kozień M.S. 2000. *Ćwiczenia laboratoryjne z miernictwa dynamicznego*. [In Polish: *Laboratory Exercises with Dynamic Measurement*.] Cracow: Wydawnictwo Politechniki Krakowskiej.
14. Litak G., M.I. Friswell. 2003. "Vibration in gear system". *Chaos, Solution and Fractals* 16: 795-800. ISSN 0960-0779
15. Łuczko Jan. 2008. *Drgania regularne i chaotyczne w nieliniowych układach mechanicznych*. [In Polish: *Regular and Chaotic Vibrations in Non-linear Mechanical Systems*.] Cracow: Wydawnictwo Politechniki Krakowskiej. ISBN 978-83-7242-492-1.
16. Mężyk Arkadiusz. 2002. "Optymalizacja własności dynamicznych układów napędowych maszyn". [In Polish: "Optimization of dynamic properties of machine drive systems".] *Zeszyty Naukowe Politechniki Śląskiej, Mechanika* 139. ISSN: 0434-0817.
17. Mężyk Arkadiusz. 2002. *Analiza i kształtowanie cech dynamicznych napędów elektromechanicznych*. [In Polish: *Analysis and Development of Dynamic Features of Electromechanical Drives*.] Gliwice: Wydawnictwo Politechniki Śląskiej. ISBN 83-7335-078-0.
18. Müller Ludwik. 1986. *Przekładnie zębate - dynamika*. [In Polish: *Toothed Gears - Dynamics*.] Warsaw: Wydawnictwa Naukowo-Techniczne. ISBN 83-204-0766-4.
19. Peiting Heinz-Otto, Saupe Dietmar. 1996. *Granice chaosu, fraktale*. [In Polish: *Limits of Chaos, Fractals*.] Warsaw: PWN. ISBN 83-0111-784-2.
20. Reszuta K., J. Drewniak. 2015. "Komputerowo wspomagane modelowanie dynamiki przekładni dwudrożnej". [In Polish: "Computer-aided modelling of two-way transmission dynamics".] *Mechanik* 7: 715-724. ISBN 0025-6552.
21. Shuang L., W. Jin-Jin, L. Jin-Jie, L. Ya-Qian. 2015. "Nonlinear parametrically excited vibration and active control of gear pair system with time-varying characteristic". *Chinese Physical Society* 214 (10). DOI: 10.1088/1674-1056/24/10/104501.
22. Wang J., J. Zheng, Z. Yang. 2012. "An analytical study of bifurcation and chaos in a spur gear pair with sliding friction". In *International Conference on Advances in Computational Modeling and Simulation, Procedia Engineering* 31: 563-570.
23. Wilk Andrzej. 1981. "Wpływ parametrów technologicznych i konstrukcyjnych na dynamikę przekładni o zębach prostych". [In Polish: "The influence of technological and construction parameters on the dynamics of gears with straight teeth".] *Zeszyty Naukowe Politechniki Śląskiej, Mechanika*, z. 72. ISSN 0434-0817.
24. Zhao X., C. Chen, J. Liu, L. Zhang. 2015. "Dynamics characteristics of a spur gear transmission system for a wind turbine". In *International Conference on Automation, Mechanical Control and Computational Engineering*: 1985-1990.

25. Zhang Y., Z. Meng, Y. Sun. 2016. "Dynamic modeling and chaotic analysis of gear transmission system in a braiding machine with or without random perturbation". *Shock and Vibration*. Article ID 8457645. ISSN 1070-9622. DOI: 10.1155/2016/8457645.

Received 19.08.2017; accepted in revised form 07.11.2017



Scientific Journal of Silesian University of Technology. Series Transport is licensed under a Creative Commons Attribution 4.0 International License